



タイトル Title	Relationship between sound radiation from sound-induced and force-excited vibration: Analysis using an infinite elastic plate model
著者 Author(s)	Yairi, Motoki / Sakagami, Kimihiro / Nishibara, Kosuke / Okuzono, Takeshi
掲載誌・巻号・ページ Citation	Journal of the Acoustical Society of America, 140(1):453-460
刊行日 Issue date	2016-07
資源タイプ Resource Type	Journal Article / 学術雑誌論文
版区分 Resource Version	publisher
権利 Rights	©2016 Acoustical Society of America. This article may be downloaded for personal use only. Any other use requires prior permission of the author and the Acoustical Society of America. The following article appeared in Journal of the Acoustical Society of America 140(1), 453-460 and may be found at http://dx.doi.org/10.1121/1.4955308 .
DOI	10.1121/1.4955308
JaLDOI	
URL	http://www.lib.kobe-u.ac.jp/handle_kernel/90003665

Relationship between sound radiation from sound-induced and force-excited vibration: Analysis using an infinite elastic plate model

Motoki Yairi^{a)}

Kajima Technical Research Institute, Chofu, Tokyo 182-0036, Japan

Kimihiro Sakagami, Kosuke Nishibara, and Takeshi Okuzono

Environmental Acoustics Laboratory, Department of Architecture, Graduate School of Engineering, Kobe University, Rokko, Nada, Kobe 657-8501, Japan

(Received 6 January 2016; revised 9 June 2016; accepted 16 June 2016; published online 20 July 2016)

Although sound radiation from sound-induced vibration and from force-excited vibration of solid structures are similar phenomena in terms of radiating from vibrating structures, the general relationship between them has not been explicitly studied to date. In particular, airborne sound transmission through walls and sound radiation from structurally vibrating surfaces in buildings are treated as different issues in architectural acoustics. In this paper, a fundamental relationship is elucidated through the use of a simple model. The transmission coefficient for random-incidence sound and the radiated sound power under point force excitation of an infinite elastic plate are both analyzed. Exact and approximate solutions are derived for the two problems, and the relationship between them is theoretically discussed. A conversion function that relates the transmission coefficient and radiated sound power is obtained in a simple closed form through the approximate solutions. The exact solutions are also related by the same conversion function. It is composed of the specific impedance and the wavenumber, and is independent of any elastic plate parameters. The sound radiation due to random-incidence sound and point force excitation are similar phenomena, and the only difference is the gradient of those characteristics with respect to the frequency. © 2016 Acoustical Society of America. [<http://dx.doi.org/10.1121/1.4955308>]

[JFL]

Pages: 453–460

I. INTRODUCTION

A. Background

Sound radiation from solid bodies due to force-excited vibration is well known as structure-borne sound, which is perceived by listeners as a consequence of airborne sound radiated from the vibrating surfaces.¹ Structure-borne sound is caused by sound-induced vibration as well as force-excited vibration, which are essentially similar phenomena in terms of radiating from vibrating solid bodies. The reduction of these two types of structure-borne sound is a fundamental issue in noise-control engineering and a basic requirement for many buildings, cars, ships, airplanes, and urban areas to realize a comfortable sound environment.²

In architectural acoustics, sound radiation from sound-induced vibration of boundaries such as walls, ceilings, and floors into rooms is generally called airborne sound transmission, and is separated from sound radiation from force-excited vibration of solid structures.³ The insulation performance of airborne sound transmission is evaluated under the assumption that the source of the excitation force is random-incidence sound, given that various angles of incidence are likely to occur in actual situations. Considering the recent increase in collective housing units and overcrowding in urban areas, the

demand for higher-performance airborne sound insulation is growing steadily. Therefore, various researchers are carrying out studies based on the considerable knowledge published so far.^{1–3} For example, Brunskog⁴ and Davy^{5,6} have presented revised theories for predicting the sound insulation of single-leaf walls and double-leaf cavity walls.

Meanwhile, the reduction of sound radiation from force-excited vibration is also a fundamental issue in architectural acoustics. Several sources of excitation force such as building facilities, railway, and road traffic vibrations, etc., contribute to sound radiation from the surfaces in actual buildings. The impact sound insulation of floors in collective housing units is also included in this issue. To predict the sound radiation from force-excited vibration of complex building structures, Asakura *et al.*⁷ solved the equations of motion for a plate theory using the finite-difference time-domain method. The governing equation used in the literature is based on the bending vibration of elastic plates driven by concentrated force excitation. The sound radiation from an elastic plate driven by point force excitation has been studied as a fundamental issue in underwater acoustics⁸ as well as architectural acoustics.

As described above, airborne sound transmission through walls and sound radiation from structurally vibrating surfaces in buildings have historically been treated as different issues in architectural acoustics only because of the different sources of excitation force. The general relationship between these

^{a)}Electronic mail: yairi@kajima.com

two issues has not been explicitly discussed except for a few studies on the particular relationship between the floor impact sound level and the floor's sound transmission loss.^{9,10} Sound radiation from sound-induced and force-excited vibration are, however, essentially similar phenomena in terms of radiating from vibrating boundaries. The coincidence effect of walls and the mass-air-mass resonance of double-leaf structures are not unique phenomena for airborne sound transmission.^{11,12}

B. Hypothesis

Considering the above background, it is important to find a general relationship between airborne sound transmission and sound radiation from force-excited vibration. If a systematic relationship exists, and can be expressed in a simple form, it would contribute significantly to the future of engineering acoustics.

Figure 1 provides a schematic explanation of the evaluation systems for airborne sound transmission and sound radiation from force-excited vibration of boundaries, and a hypothesis on the relationship between the two problems. M_a and M_s indicate the evaluation index for each problem. The reduction index, which is the reciprocal of the transmission coefficient for random-incidence sound represented in dB scale, is widely used for M_a in architectural acoustics. When a wall is excited by a small sound source nearby, it is expected to be driven not by a plane wave but by a spherical wave.^{13,14} In this case, the reduction index of a spherical wave incidence is applicable to M_a . The radiation coefficient and radiation impedance are widely used for M_s .¹⁵⁻¹⁷ Insulation performance for the floor impact noise is also used as M_s . The relationship between M_a and M_s in the following expressions is defined using a linear operator, ϵ :

$$\begin{cases} M_a = \epsilon [M_s] \\ M_s = \epsilon^{-1} [M_a] \end{cases} \quad (1)$$

To be able to estimate the airborne sound transmission from the sound radiation characteristics, or vice versa, ϵ should exist in a form independent of the boundaries. The chief

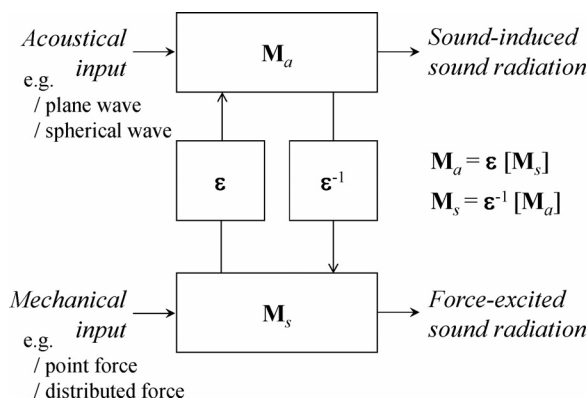


FIG. 1. Schematic explanation of evaluation systems for sound radiation from sound-induced and force-excited vibration of boundaries, and a hypothesis on the relationship between them.

purpose of the present work is to determine the possible existence of such a linear operator.

In this paper, the sound radiation from an infinite elastic plate driven by random-incidence sound and point force excitation is theoretically investigated. The transmission coefficient for random-incidence sound and the radiated sound power under point force excitation are introduced for M_a and M_s , respectively, and these exact solutions are both derived. Approximate solutions of M_a and M_s are both analyzed within the low-frequency limit under the critical frequency without acoustic loading. Then, a conversion function that relates the two problems is derived through the approximate solutions, and its accuracy and dependence on the elastic plate are discussed. Physical meanings of the conversion function are also given. Finally, numerical calculations are used to verify if the conversion function is also applicable to the relationship between the exact solutions.

II. TRANSMISSION COEFFICIENT FOR RANDOM-INCIDENCE SOUND

A. Exact solution

Consider an infinite elastic plate lying in the plane $z = 0$ (Fig. 2), which vibrates under a plane wave incident at the angle Θ . Suppose that the vibration of the plate is in accordance with the classic thin plate theory and the acoustic admittance of both sides of the plate is zero, i.e., no absorption. The transmitted sound field is derived by simultaneously solving the governing equations of the sound field and the equation of motion of the plate. In this case, the transmission coefficient for oblique-incidence sound, $\tau_{\Theta}(\omega)$, is defined by the ratio of an incidence sound at the angle Θ and the transmitted sound at the same angle. This problem has been solved previously, and the exact solution of $\tau_{\Theta}(\omega)$ is written as follows:²

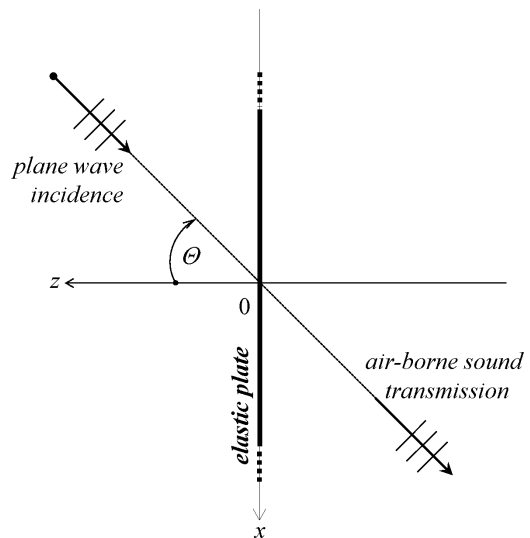


FIG. 2. Analytical model of an infinite elastic plate in accordance with the thin plate theory, which vibrates and radiates sound driven by an oblique plane wave incident.

$$\tau_{\Theta}(\omega) = \left[\left(1 + \eta \frac{\omega \rho_p h \cos \Theta}{2 \rho_0 c_0} \frac{\omega^2 \text{Re}[D] \sin^4 \Theta}{c_0^4 \rho_p h} \right)^2 + \left(\frac{\omega \rho_p h \cos \Theta}{2 \rho_0 c_0} \right)^2 \left(1 - \frac{\omega^2 \text{Re}[D] \sin^4 \Theta}{c_0^4 \rho_p h} \right)^2 \right]^{-1}, \quad (2)$$

where ω is the angular frequency, c_0 is the speed of sound in air, ρ_0 is the air density, and $D = E(1 - i\eta)h^3/12(1 - \nu^2)$ is the flexural rigidity of the plate with E being Young's modulus, h thickness, η loss factor, ν Poisson's ratio, and ρ_p density of the plate. The angle of incidence affects the bending vibration of the plate, which is well known as the coincidence effect. $\omega_c = (c_0^4 m / \text{Re}[D])^{1/2}$ is the critical frequency. When an elastic plate is accompanied by bending vibrations due to oblique plane-wave incidence, the transmission coefficient becomes larger than that of normal plane-wave incidence above the critical frequency. A fundamental theory for the range above the critical frequency has been established,¹⁸ and a number of researchers have developed it further.^{5,19}

The transmission coefficient for random-incidence sound is defined as the ratio of the transmitted sound power to the incident sound power from any direction. Random incidence is obtained by averaging the transmission coefficients for oblique incidence over a hemisphere. This approach, which is based on a completely diffuse sound field, does not fully reflect the actual conditions in rooms, and so various methods of truncating the angle of incidence up to a certain limit angle have been proposed.^{2,20} In general, this is calculated by integrating a range of $\Theta = 0^\circ - 78^\circ$ because of the good agreement with experimental results.^{2,3} The transmission coefficient for random-incidence sound, $\tau_f(\omega)$, is therefore derived from the following integration:

$$\tau_f(\omega) = \frac{\int_0^{78} \tau_{\Theta}(\omega) \cos \Theta \sin \Theta d\Theta}{\int_0^{78} \cos \Theta \sin \Theta d\Theta}. \quad (3)$$

B. Approximate solution

The integral in Eq. (3) is evaluated analytically within the low-frequency limit when $\text{Re}[D]$ is negligible,

$$\tau_{\Theta}(\omega) \cong \left(\frac{2 \rho_0 c_0}{m \omega \cos \Theta} \right)^2 \left[1 + \left(\frac{m \omega \cos \Theta}{2 \rho_0 c_0} \right)^2 \right]^{-1}. \quad (4)$$

$m = \rho_p h$ is the surface density of the plate. The approximate solution of the transmission coefficient for random-incidence sound, $\hat{\tau}_f(\omega)$, is then derived by substituting Eq. (4) into Eq. (3),

$$\hat{\tau}_f(\omega) \cong \frac{\ln \left[1 + \left(\frac{m \omega}{2 \rho_0 c_0} \right)^2 \right] - \ln \left[1 + 0.04 \left(\frac{m \omega}{2 \rho_0 c_0} \right)^2 \right]}{\left(\frac{m \omega}{2 \rho_0 c_0} \right)^2}. \quad (5)$$

The terms in square brackets in Eq. (4) denote the effect of acoustic loading. If this is ignored, it can be further simplified

$$\tau_{\Theta}(\omega) \cong \left(\frac{2 \rho_0 c_0}{m \omega \cos \Theta} \right)^2. \quad (6)$$

In this case, $\hat{\tau}_f(\omega)$ is derived by substituting Eq. (6) into Eq. (3) as well,

$$\hat{\tau}_f(\omega) = 3.28 \left(\frac{2 \rho_0 c_0}{m \omega} \right)^2 \cong 3.28 \tau_0(\omega), \quad (7)$$

where $\tau_0(\omega)$ is the transmission coefficient for normal-incidence sound. The transmission coefficient for random-incidence sound is known to be approximately represented in relation to the transmission coefficient for normal-incidence sound.² It is usually expressed in the form of a sound transmission loss in dB scale by taking the logarithm of its reciprocal as

$$10 \log[1/\hat{\tau}_f(\omega)] \cong 10 \log[1/\tau_0(\omega)] - 5 \text{ dB}. \quad (8)$$

The reduction index is proportional to both the frequency and the surface density of the plate. This is called the "mass law" for random-incidence sound. Doubling the weight of the wall or the frequency gives an increase of 6 dB. The mass law is a fundamental principle for airborne sound insulation of walls, and is widely used in actual engineering situations.

Numerical examples of Eqs. (3) and (7) are shown in Fig. 3. The two characteristics are in good agreement with each other in the low-frequency range below the critical frequency. Note that they differ slightly at very low frequencies because the effect of acoustic loading is ignored.

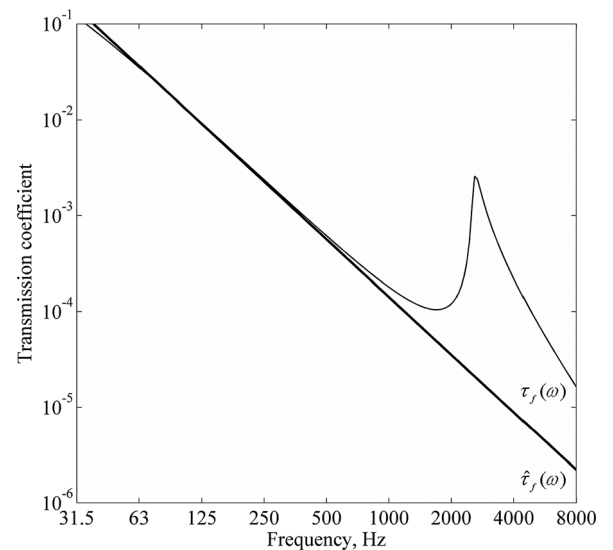


FIG. 3. Numerical example of the transmission coefficient for random-incidence sound: Comparison of the approximate solution, $\hat{\tau}_f(\omega)$, in Eq. (7) (thick line) and the exact solution, $\tau_f(\omega)$ in Eq. (3) (thin line) in the case of $\rho_p = 1000 \text{ kg/m}^3$, $h = 20 \text{ mm}$, $E = 1.8 \times 10^9 \text{ N/m}^2$, $\eta = 0.03$, and $\nu = 0.3$.

III. RADIATED SOUND POWER UNDER POINT FORCE EXCITATION

A. Exact solution

Consider an infinite elastic plate lying in the plane $z=0$ (Fig. 4), which vibrates driven by point force excitation. Suppose that the vibration of the plate is in accordance with the classic thin plate theory and the acoustic admittance of both sides of the plate is zero, i.e., no absorption. The radiated sound power is derived by simultaneously solving the governing equations of the sound field and the equation of motion of the plate. The effects of acoustic loading on both sides of the plate are taken into account in this model (cf. Junger and Feit⁸ assume that the effects of acoustic loading on one side of the plate are zero). Considering the problem as being axisymmetrical and using the Hankel transform technique in cylindrical coordinates, the sound pressure on the plate, $p(r_0)$, and the angular spectrum, $W(k)$, with respect to the displacement of the plate, $w(r_0)$, are obtained and expressed as follows:

$$p(r_0) = \rho_0 \omega^2 \int_0^\infty \frac{W(k)}{\sqrt{k^2 - k_0^2}} J_0(kr) k dk, \quad (9)$$

$$W(k) = -\frac{1}{2\pi} \frac{1}{\frac{2\rho_0 \omega^2}{\sqrt{k^2 - k_0^2}} - (Dk^4 - \rho_p h \omega^2)}, \quad (10)$$

where k_0 is the acoustic wavenumber in the air and $w(r_0)$ and $W(k)$ are related to the Hankel transform defined by the following equations:

$$\begin{cases} W(k) = \int_0^\infty w(r) J_0(kr) r dr \\ w(r) = \int_0^\infty W(k) J_0(kr) k dk. \end{cases} \quad (11)$$

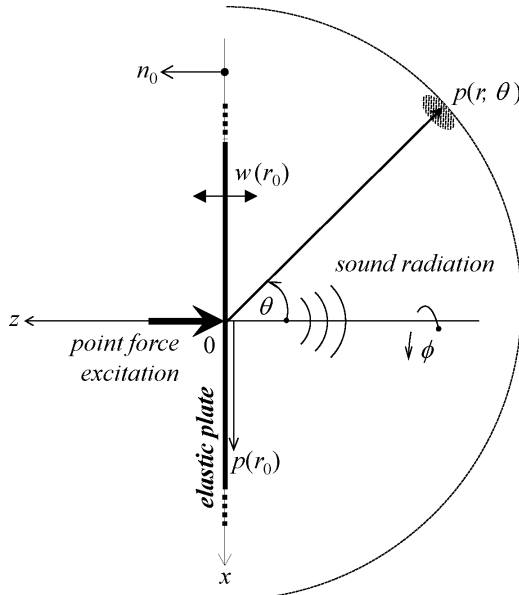


FIG. 4. Analytical model of an infinite elastic plate in accordance with the thin plate theory, which vibrates and radiates sound driven by point force excitation.

The exact solution of the radiated sound power under point force excitation, $\Pi(\omega)$, is obtained by integrating the surface intensity of the plate over the entire surface to an infinite extent, thus,

$$\Pi(\omega) = \iint_S \operatorname{Re} \left[\frac{1}{2} p(r_0) \bar{v}(r_0) \right] dS_0, \quad (12)$$

where $v(r_0) = -i\omega w(r_0)$ is the velocity of the plate with a complex conjugate. Substituting Eqs. (9) and (10) into Eq. (12), $\Pi(\omega)$ is finally expressed by the following integral:¹³

$$\begin{aligned} \Pi(\omega) &= \pi \rho_0 \omega^3 \operatorname{Re} \left[\int_0^\infty dk \int_0^\infty dk' \frac{W(k) \hat{W}(k')}{\sqrt{k_0^2 - k^2}} k k' \right. \\ &\quad \left. \times \int_0^\infty J_0(kr) J_0(k'r) r dr \right] \\ &= \pi \rho_0 \omega^3 \operatorname{Re} \left[\int_0^\infty dk \int_0^\infty \frac{W(k) \hat{W}(k')}{\sqrt{k_0^2 - k^2}} \delta(k - k') dk' \right] \\ &= \pi \rho_0 \omega^3 \int_0^{k_0} \frac{|W(k)|^2}{\sqrt{k_0^2 - k^2}} k dk, \end{aligned} \quad (13)$$

where the integral for the Dirac delta function is used²¹

$$k' \int_0^\infty J_0(kr) J_0(k'r) r dr = \delta(k - k'). \quad (14)$$

B. Approximate solution

The radiated sound power under point force excitation is also obtained by integrating the radial intensity in the far-field.^{11,12} In Fig. 4, θ denotes the polar angle between the direction of the receiving point and the negative direction of the z axis. Using Rayleigh's integral,⁸ the approximate solution of the radiated sound pressure, $p(r, \theta)$, is obtained in a closed form

$$\begin{aligned} p(r, \theta) &\cong \rho_0 \omega^2 W(k_0 \sin \theta) \frac{e^{ik_0 r}}{r} \\ &= \frac{-2i\rho_0 \omega^2}{\frac{2\rho_0 c_0 \omega}{\cos \theta} + i(Dk_0^4 \sin^4 \theta - m\omega^2)} \frac{e^{ik_0 r}}{4\pi r}. \end{aligned} \quad (15)$$

Integrating the radial intensity, $|p(r, \theta)|/2\rho_0 c_0$, over a hemisphere of radius r yields the approximate solution of the radiated sound power under point force excitation, $\hat{\Pi}(\omega)$; thus,

$$\hat{\Pi}(\omega) \cong \frac{r^2}{2\rho_0 c_0} \int_0^{2\pi} d\phi \int_0^{\pi/2} |p(r, \theta)|^2 \sin \theta d\theta. \quad (16)$$

Here further approximations are introduced. Using the coincidence frequency, $\omega_c = (c_0^4 m / \operatorname{Re}[D])^{1/2}$, Eq. (15) is rewritten as follows:

$$p(r, \theta) \cong \frac{-2i\rho_0 \omega^2}{\frac{2\rho_0 c_0 \omega}{\cos \theta} + i\left(m \frac{\omega^2}{\omega_c^2} \sin^4 \theta - m\right)} \frac{e^{ik_0 r}}{4\pi r}. \quad (17)$$

The integral in Eq. (16) is evaluated analytically within the low-frequency limit when ω^2/ω_c^2 is negligible. The approximate solution of the radiated sound power, $\hat{\Pi}(\omega)$, is therefore obtained in a closed form

$$\begin{aligned}\hat{\Pi}(\omega) &= \frac{\pi r^2}{\rho_0 c_0} \int_0^{\pi/2} \left| \frac{-2i\rho_0\omega^2}{\cos\theta} \frac{e^{ik_0 r}}{-im\omega^2} \frac{4\pi r}{4\pi r} \right|^2 \sin\theta d\theta \\ &= \frac{1}{4\pi\rho_0 c_0} \left(\frac{\rho_0}{m} \right)^2 \left[1 - \frac{2\rho_0 c_0}{m\omega} \tan^{-1} \frac{m\omega}{2\rho_0 c_0} \right].\end{aligned}\quad (18)$$

The terms in square brackets indicate the effects of acoustic loading. If these effects are negligible as in Sec. II, Eq. (18) is further simplified, finally yielding

$$\hat{\Pi}(\omega) \cong \frac{1}{4\pi\rho_0 c_0} \left(\frac{\rho_0}{m} \right)^2. \quad (19)$$

In this equation, the characteristics of the radiated sound power under point force excitation are different from the transmission coefficient for random-incidence sound, namely, the radiated sound power is reduced in 6 dB by doubling the surface density of the elastic plate but does not depend on the frequency.

Calculated examples of Eqs. (13) and (19) are shown in Fig. 5. The two characteristics are in good agreement with each other in the low-frequency range below the critical frequency. Note that both of them differ slightly at very low frequencies because the effect of acoustic loading is ignored.

IV. RELATIONSHIP BETWEEN THE TWO PROBLEMS

A. Derivation of conversion function

From the approximate solutions of the transmission coefficient for random-incidence sound, $\hat{\tau}_f(\omega)$, in Eq. (7)

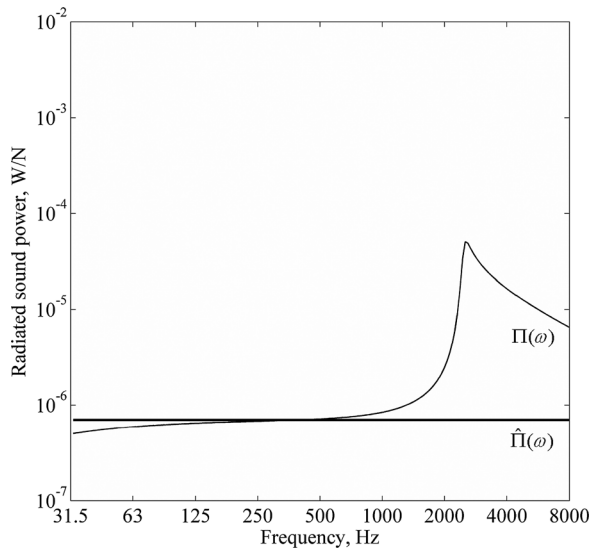


FIG. 5. Numerical example of the radiated sound power driven by point force excitation: Comparison of the approximate solution, $\hat{\Pi}(\omega)$, in Eq. (19) (thick line) and the exact solution, $\Pi(\omega)$, in Eq. (13) (thin line) in the case of $\rho_p = 1000 \text{ kg/m}^3$, $h = 20 \text{ mm}$, $E = 1.8 \times 10^9 \text{ N/m}^2$, $\eta = 0.03$, and $\nu = 0.3$.

and the radiated sound power under point force excitation, $\hat{\Pi}(\omega)$, in Eq. (19), the following relation is derived:

$$\hat{\tau}_f(\omega) = \varepsilon(\omega) \hat{\Pi}(\omega), \quad (20)$$

where the conversion function, $\varepsilon(\omega)$ is as follows:

$$\varepsilon(\omega) \cong \frac{52\pi\rho_0 c_0}{k_0^2}. \quad (21)$$

$\varepsilon(\omega)$ is a function of the specific impedance, $\rho_0 c_0$, and the wave number, k_0 , of the medium, and does not include any elastic plate parameters. This fact means that the linear operator, ε , defined in Eq. (1), exists in a form independent of the elastic plate within the low-frequency limit below the critical frequency without acoustic loading. The characteristics of $\varepsilon(\omega)$ as a function of frequency are shown in Fig. 6.

B. Effect of acoustic loading

Acoustic loading reduces the radiation efficiency of vibrating surfaces. In general, the effects of acoustic loading are negligible when the surface density of an elastic plate, m , and the angular frequency, ω , are sufficiently large, whereas those effects increase with the decrease of m and ω . The effects of acoustic loading for the two problems are calculated by Eq. (5)/Eq. (7) and Eq. (18)/Eq. (19), respectively. Figure 7 shows the calculated results as a function of frequency.

The difference in these effects between the two cases increases with the decrease of $m\omega$. As described above, the conversion function, $\varepsilon(\omega)$, is derived from approximate solutions that ignore the acoustic loading. Thus, large errors probably occur in regions in which the effects of acoustic loading cannot be ignored when the conversion function is applied to the relationship between the exact solutions. This is also discussed in Sec. IV D.

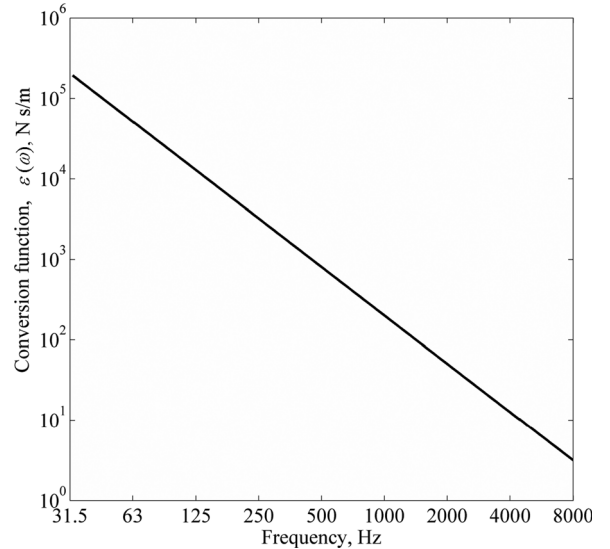


FIG. 6. Frequency characteristics of the conversion function, $\varepsilon(\omega)$, in Eq. (21).

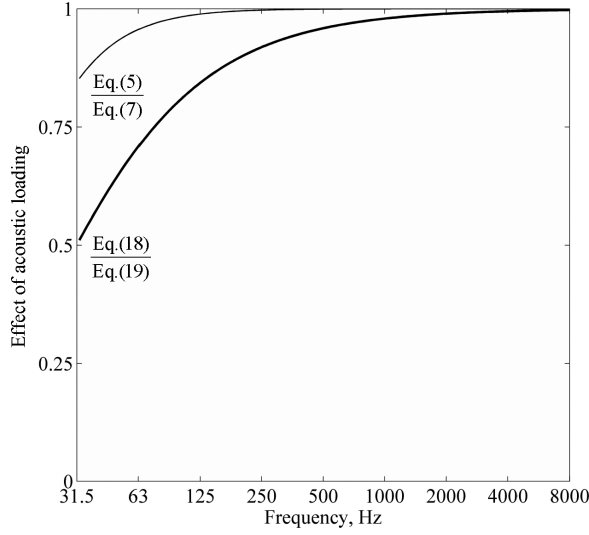


FIG. 7. Comparison of the effect of acoustic loading calculated by Eq. (5)/Eq. (7) (thin line) and Eq. (18)/Eq. (19) (thick line) in the case of $m = 10 \text{ kg/m}^2$.

C. Theoretical considerations

Consider a physical meaning of the conversion function.²² Introducing the driving point impedance, $z_p = 8(\text{Re}[D]m)^{1/2}$, into the relationship of Eq. (20), the equation is transformed to

$$\hat{\tau}_f(\omega) = \psi \frac{\hat{\Pi}(\omega)}{\frac{1}{2z_p}}, \quad (22)$$

where

$$\psi = \frac{\varepsilon(\omega)}{2z_p} = \frac{26\pi\rho_0 c_0}{k_0^2 z_p}. \quad (23)$$

The right side of Eq. (22) is expressed by the ratio of the input power under point force excitation, $1/2z_p$, and the output power, $\hat{\Pi}(\omega)$, multiplied by the factor ψ . The input–output power ratio is a dimensionless evaluation index as well as the transmission coefficient for random-incidence sound. The factor ψ in Eq. (23) is also dimensionless and is composed of the driving point impedance (\approx input impedance) and the specific impedance of the air (\approx radiation impedance).

Note that ψ depends on the parameters of the elastic plate since it includes the driving point impedance, z_p . When the input–output power ratio is used as the evaluation index \mathbf{M}_s for the sound radiation from force-excited vibration in Fig. 1, the linear operator ε is not determined in a form independent of the elastic plate. The relationship between the transmission coefficient for random-incidence sound and the input–output power ratio for point force excitation expressed by Eq. (22) is shown in Fig. 8.

D. Application of the conversion function to the exact solutions

The conversion function, $\varepsilon(\omega)$, derived through the discussions so far is obtained under the relationship between the approximate solutions so it is not clear whether $\varepsilon(\omega)$ is

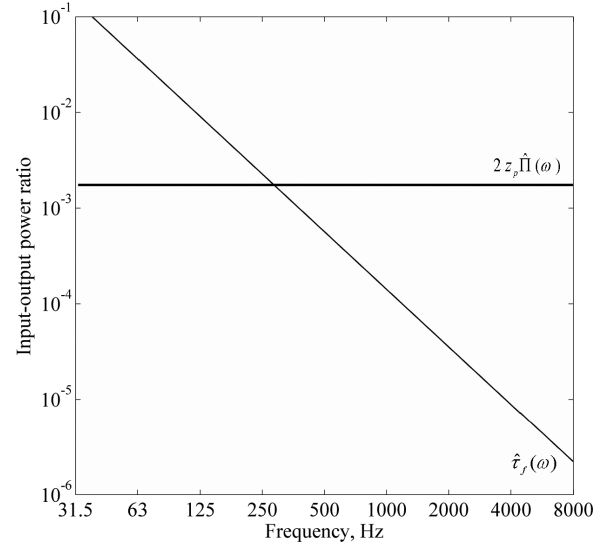


FIG. 8. Comparison of the input–output power ratio driven by random-incidence sound (thin line) and point force excitation (thick line) in the case of $\rho_p = 1000 \text{ kg/m}^3$, $h = 20 \text{ mm}$, $E = 1.8 \times 10^9 \text{ N/m}^2$, $\eta = 0.03$, and $\nu = 0.3$.

applicable to the relationship between the exact solutions. In this section, the possibility of the application of $\varepsilon(\omega)$ to the exact solutions, namely,

$$\tau_f(\omega) \cong \varepsilon(\omega) \Pi(\omega), \quad (24)$$

is verified by numerical calculations. Note that the exact solutions, $\tau_f(\omega)$ and $\Pi(\omega)$, are shown in Eqs. (3) and (13), respectively.

Two kinds of elastic plates used in the calculations are shown in Table I. These are assumed to be typical building materials: gypsum board (12.5 mm in thickness) and reinforced concrete panel (250 mm in thickness). In the calculations, the reciprocal of both terms in Eq. (24) are represented and compared in dB scale; thus, $10\log_{10}[1/\tau_f(\omega)]$ and $10\log_{10}[1/\varepsilon(\omega)\Pi(\omega)]$. Figure 9 shows the calculated results, which exhibit similar tendencies. The typical behavior is characterized by a significant dip around the critical frequency, which is caused by the coincidence effect of the plate. $10\log_{10}[1/\tau_f(\omega)]$ and $10\log_{10}[1/\varepsilon(\omega)\Pi(\omega)]$ are in fairly good agreement with each other at all frequencies. The differences are largest around the critical frequency, but are within 2 dB. The effect of ignoring the acoustic loading is also small.

Thus, it was shown that the exact solutions of both problems were also related by the same conversion function, $\varepsilon(\omega)$, at all frequencies including above the critical frequency. This fact suggests that the sound radiation from an infinite elastic

TABLE I. Physical parameters of elastic plates used in the calculations.

Parameters	Gypsum board	Reinforced concrete
Young's modulus, E , N/m^2	1.8×10^9	2.6×10^{10}
Thickness, h , m	0.013	0.25
Loss factor, η	0.03	0.005
Poisson's ratio, ν	0.3	0.2
Density, ρ_p , kg/m^3	650	2400

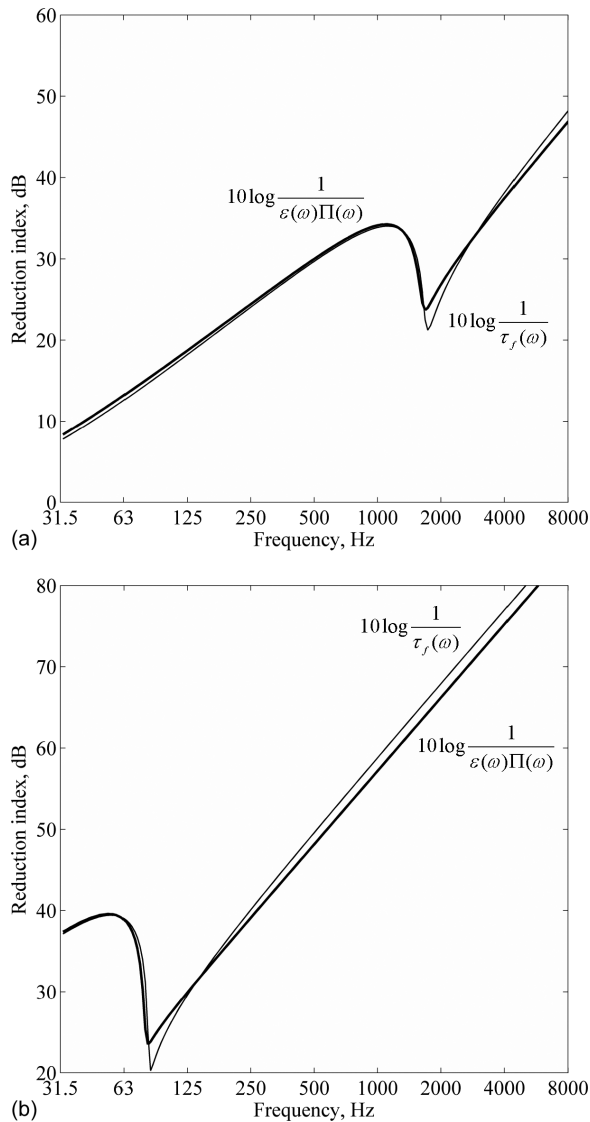


FIG. 9. Application of the conversion function, $\varepsilon(\omega)$, to the exact solutions: The exact solutions, $\tau_f(\omega)$ (thin line) and $\Pi(\omega)$ multiplied by $\varepsilon(\omega)$ (thick line) are numerically compared. The calculated results are shown in the forms of those reciprocals in dB scale in the case of gypsum board (a) and reinforced concrete (b).

plate with random-incidence sound and point force excitation are essentially similar phenomena, and the only difference is the gradient of those characteristics in dB scale with respect to the frequency. The possible extension of the conversion function to finite plates is in a future plan.

V. CONCLUSIONS

In order to acquire fundamental insight into the relationship between airborne sound transmission and sound radiation from force-excited vibration of solid structures, theoretical studies were carried out using an infinite elastic plate model. In this paper, random-incidence sound and point force excitation were introduced into the analysis as the source of external force for each problem. Exact solutions of the transmission coefficient for random-incidence sound and radiated sound power under point force excitation were shown. Approximate solutions of those problems were

both derived from the exact solutions within the low-frequency limit below the critical frequency without acoustic loading.

A conversion function that relates the two problems was obtained in a simple closed form through the approximate solutions. Numerical calculations verified that the conversion function is applicable to the relationship between the exact solutions. It was shown that the exact solutions of both problems were also related by the same conversion function at all frequencies including above the critical frequency, and the effect of ignoring the acoustic loading was sufficiently small as well. The conversion function is composed of only the specific impedance and the wavenumber of the medium and does not include any elastic plate parameters, namely, the linear operator that relates sound-induced and force-excited sound radiation defined in this paper exists in a form independent of an infinite elastic plate. This fact suggests that the airborne sound insulation for random-incidence sound can be estimated from the radiated sound power under point force excitation, or vice versa, without knowing any parameters of the single-leaf walls in buildings. A physical meaning for the conversion function was also given by introducing the driving point impedance of point force excitation into the relationship.

All findings of the present work suggest that the sound radiation from an infinite elastic plate due to random-incidence sound (sound-induced vibration) and point force excitation (force-excited vibration) are essentially similar phenomena, and the only difference between them is the overall gradient of those characteristics in dB scale with respect to the frequency.

¹L. Cremer, M. Heckl, and B. A. T. Petersson, *Structure-Borne Sound: Structural Vibrations and Sound Radiation at Audio Frequencies*, 3rd ed. (Springer, Berlin, 2005), Chap. 1.

²L. L. Beranek and I. L. Vér, *Noise and Vibration Control Engineering: Principles and Applications* (John Wiley and Sons, New York, 1992), Chap. 11.

³Z. Maekawa, J. H. Rindel, and P. Lord, *Environmental and Architectural Acoustics*, 2nd ed. (CRC Press, New York, 2011), Chap. 5.

⁴J. Brunsog, "The forced sound transmission of finite single leaf walls using a variational technique," *J. Acoust. Soc. Am.* **132**, 1482–1493 (2012).

⁵J. L. Davy, "Predicting the sound insulation of single leaf walls: Extension of Cremer's model," *J. Acoust. Soc. Am.* **126**, 1871–1877 (2009).

⁶J. L. Davy, "The improvement of a simple theoretical model for the prediction of the sound insulation of double leaf walls," *J. Acoust. Soc. Am.* **127**, 841–849 (2010).

⁷T. Asakura, T. Ishizuka, T. Miyajima, M. Toyoda, and S. Sakamoto, "Prediction of low-frequency structure-borne sound in concrete structures using the finite-difference time-domain method," *J. Acoust. Soc. Am.* **136**, 1085–1100 (2014).

⁸M. Junger and D. Feit, *Sound, Structures, and Their Interaction* (MIT Press, Cambridge, MA, reprinted by the Acoustical Society of America, 1993), Chap. 8.

⁹M. Yairi and E. J. Rathe, "Relationship between the transmission loss and the impact-noise isolation of floor structures," *J. Acoust. Soc. Am.* **35**, 1825–1830 (1963).

¹⁰I. L. Vér, "Relation between the normalized impact sound level and sound transmission loss," *J. Acoust. Soc. Am.* **50**, 1414–1417 (1971).

¹¹M. Yairi, K. Sakagami, M. Morimoto, A. Minemura, and K. Andow, "Sound radiation from a double-leaf elastic plate with a point force excitation: Effect of an interior panel on the structure-borne sound radiation," *Appl. Acoust.* **63**, 737–757 (2002).

¹²M. Yairi, K. Sakagami, M. Morimoto, A. Minemura, and K. Andow, "Effect of acoustical damping with a porous absorptive layer in the cavity

- to reduce the structure-borne sound radiation from a double-leaf structure,” *Appl. Acoust.* **64**, 365–384 (2003).
- ¹³D. Takahashi, Y. Furue, and K. Matsuura, “Vibration and sound transmission of an elastic plate by a spherical sound wave,” *J. Acoust. Soc. Jpn. (J)* **35**, 314–321 (1979) (in Japanese with English abstract). The sound insulation for spherical wave incidence is analyzed and numerical examples are given. It is shown that the reduction index for the spherical wave incidence is lower than that for the plane wave incidence.
 - ¹⁴M. Yairi, T. Koga, K. Takebayashi, and K. Sakagami, “Transmission of a spherical sound wave through a single-leaf wall: Mass law for spherical wave incidence,” *Appl. Acoust.* **75**, 67–71 (2014).
 - ¹⁵K. Gösele, “Zur Bewertung der Schalldämmung von Batwteilen nach solkurven” (“Evaluating the sound insulation of buildings according to theoretical curves”), *Acustica* **15**, 264–270 (1965). For the appraisal of the reduction of impact noise transmitted through ceilings and of the airborne sound-damping of walls and ceilings, in Germany the measurements are compared with the theoretical curves in accordance with DIN 52211.
 - ¹⁶G. Maidanik, “Response of ribbed panels to reverberant acoustic fields,” *J. Acoust. Soc. Am.* **34**, 809–826 (1962).
 - ¹⁷M. C. Gomperts, “Sound radiation from baffled thin rectangular plates,” *Acustica* **37**, 93–102 (1977).
 - ¹⁸L. Cremer, “Theory of the sound attenuation of thin walls with oblique incidence,” in *Architectural Acoustics, Benchmark Papers in Acoustics*, edited by T. D. Northwood (Dowden, Hutchinson and Ross, Stroudsburg, PA, 1977), pp. 367–399.
 - ¹⁹S. Ljunggren, “Airborne sound insulation of thick walls,” *J. Acoust. Soc. Am.* **89**, 2338–2345 (1991).
 - ²⁰H. Kang, J. Ih, J. Kim, and H. Kim, “Prediction of sound transmission loss through multilayered panels by using Gaussian distribution of directional incident energy,” *J. Acoust. Soc. Am.* **107**, 1413–1420 (2000).
 - ²¹P. M. Morse and H. Feshbach, *Methods of Theoretical Physics Part 1* (McGraw-Hill, New York, 1953), Chap. 13.
 - ²²M. Yairi, K. Sakagami, K. Nishibara, and T. Okuzono, “On the relationship between the normal incidence airborne sound-excited and the structurally-excited sound radiation from a wall: A theoretical trial with simplified models,” *J. Build. Acoust.* **22**, 109–122 (2015).